ORIGINAL PAPER

CrossMark

NKG2D ligands in glioma stem-like cells: expression in situ and in vitro

Charlotte Flüh[1] · Guranda Chitadze[2] · Vivian Adamski[1] · Kirsten Hattermann[3] · Michael Synowitz[1] · Dieter Kabelitz[2] · Janka Held-Feindt[1]

Abstract

Glioblastoma multiforme (GBM) is a highly malignant brain tumor. Tumor stem cells have a major influence on tumor malignancy, and immunological escape mechanisms, involving the Natural Killer Group 2, member D (NKG2D) receptor-ligand-system, are key elements in tumor immuno-surveillance. We analyzed the expression profile and localization of NKG2D ligands (NKG2DL) and embryonic and neural stem cell markers in solid human GBM and stem-like cells isolated from glioma cell lines by qRT-PCR and immunohistochemistry, including quantitative analysis. We also evaluated the effect of Temozolomide (TMZ), the standard chemotherapeutic agent used in GBM therapy, on NKG2DL expression. NKG2DL-positive cells were mostly found scattered and isolated, were detectable in glial fibrillary acidic protein (GFAP)-positive tumor regions and partly in the penumbra of tumor vessels. NKG2DL were found in a distinct tumor stem-like cell subpopulation and were broadly costained with each other. Quantitative analysis revealed, that dependent on the individual NKG2DL investigated, cell portions costained with different stem cell markers varied between small (Musashi-1) and high (KLf-4) amounts. However, a costaining of NKG2DL with CD3γ, typically found in T cells, was also observable, whereas CD11b as a marker for tumor micoglia cells was only rarely costained with NKG2DL. Stem-like cells derived from the glioma cell lines T98G and U251MG showed a distinct expression pattern of NKG2DL and stem cell markers, which seemed to be balanced in a cell line-specific way. With differentiation, T98G displayed less NKG2DL, whereas in U251MG, only expression of most stem cell markers decreased. In addition, stimulation with TMZ led to a significant upregulation of NKG2DL in stem-like cells of both lines. As stem-like glioma cells tend to show a higher expression of NKG2DL than more differentiated tumor cells and TMZ treatment supports upregulation of NKG2DL, the NKG2D system might play an important role in tumor stem cell survival and in GBM therapy.

Keywords Glioblastoma · NKG2DL · MICA · MICB · Stem cells · Temozolomide

---

Charlotte Flüh and Guranda Chitadze have contributed equally.

✉ Charlotte Flüh
  charlotte.flueh@uksh.de

1   Department of Neurosurgery, University Medical Center Schleswig-Holstein, Campus Kiel, Arnold-Heller-Straße 3, Haus 41, 24105 Kiel, Germany

2   Institute of Immunology, University Medical Center Schleswig-Holstein, Campus Kiel, Arnold-Heller-Straße 3, Haus 17, 24105 Kiel, Germany

3   Institute of Anatomy, Christian-Albrechts-University, Olshausenstraße 40, 24098 Kiel, Germany

Introduction

Glioblastoma multiforme (GBM) is the most common primary brain tumor in adults. Standard therapy includes resection and aggressive radiochemotherapy. The overall survival remains extremely low with an average of 14 months (Stupp et al. 2009). This points to the urgent need of new therapeutic approaches.

One reason for the resistance against the current treatment options might be the heterogeneity of glioblastomas (Sottoriva et al. 2013; Aum et al. 2014). Glioma heterogeneity is represented on genetic, hierarchical, functional, and epigenetic levels (Bassoy et al. 2016), resulting in a poor responsiveness to different therapeutic approaches (Bao et al. 2006; Kreso and Dick 2014). Since an extensive analysis of various neural and embryonal stem cell markers showed that a

master marker for glioma stem cells is missing (Fluh et al. 2016), not only differentiated tumor cells, but also tumor cells with stem cell properties show a distinct heterogeneity. As the proportion of tumor stem cells is closely associated with the aggressiveness and with a bad prognosis in GBM, tumor stem cells and especially the understanding of their heterogeneous phenotypes are of high interest concerning treatment of glioblastomas (Zeppernick et al. 2008).

Following the concept of the stem cell hypothesis, stem cells have tumor-initiating potential, are pluripotent, show resistance to chemo-therapy, and are, therefore, key elements in tumor progression and recurrence. Concerning gliomas, specific characteristics of tumor stem cells, including, e.g., expression of the neural and embryonic stem cell markers like Klf-4 (Krüppel-like factor 4), Oct-4 (octamer binding transcription factor; synonymous Oct-3, POU5F1), Sox-2 (sex determining region Y-box 2), Nanog (Tir nan Og), and Musashi-1 [RNA-binding protein Musashi homolog 1 (*Drosophila*)] have been studied extensively by us and others (Bradshaw et al. 2016; Hattermann et al. 2016).

Although the molecular mechanisms causing the ineffi- cacy of current treatment strategies are, to date, not fully identified, an important system of recognition and potential elimination of tumor (stem) cells is provided by the Natu- ral Killer Group 2D (NKG2D) system. Facing challenging environmental conditions, malignant glioma cells express several stress inducible molecules like the Natural Killer Group 2D ligands (NKG2DL), which are recognized by the NKG2D receptor (Jung et al. 2013; Chitadze et al. 2017). NKG2DL are usually not expressed on healthy cells, but are induced in response to different types of cellular stress, such as viral infection, genotoxic stress, or malignant transforma- tion (Nausch and Cerwenka 2008). There are eight different NKG2DL known: MHC class I chain-related proteins A and B (MICA and MICB) and six members of the UL16-binding protein family [ULBP1-6; (Raulet et al. 2013)]. Interaction between NKG2DL and the receptor, which is typically located on effector cells of the immune system like NK cells, NK T cells, gamma delta T cells, CD8 positive T cells, and a minor subset of immune regulatory CD4-positive T cells (Chitadze et al. 2015), triggers cytotoxicity in NK cells, and induces costimulation of T-cell subsets (Champsaur and Lanier 2010), which usually results in killing of the NKG2DL carrying cell. As a mechanism of immuno-sur- veillance, tumor cells may release soluble NKG2DL (sNK- G2DL) or process membrane-bound NKG2DL in exosomes (Chitadze et al. 2013). Thus, high serum levels of NKG2DL are associated with a bad prognosis and short survival in many malignancies like breast or pulmonary cancer (Salih et al. 2008). It was shown by us and others that NKG2DL are expressed on human GBM cells and corresponding glioma cell lines (Lamb et al. 2013), and that cytotoxic activity of gamma delta T cells towards glioma cells is enhanced in a

NKG2D and T-cell receptor (TCR)-dependent manner (Chi- tadze et al. 2015).

NKG2DL are not only present on differentiated tumor cells, but also on induced pluripotent stem cells (Kruse et al. 2015) and induced pluripotent glioma stem cells (Wolpert et al. 2014). Di Tomaso et al. did not find any differences in NKG2DL expression when comparing glioma stem cells and corresponding differentiated cells derived from human glio- blastoma patients (Di Tomaso et al. 2010). In contrast, Codo et al. found a lower expression of NKG2DL in stem-like glioma cell lines compared to differentiated glioma cell lines (Codo et al. 2014). Interestingly, immunogenicity of glioma stem cells might depend on the glioma subtype (Beier et al. 2012). However, detailed information on the distribution of various NKG2DL in different subpopulations of the hetero- geneous glioma stem cell compartment and on the effect of chemotherapeutic treatment on NKG2DL expression espe- cially in glioma stem cells is still lacking.

Thus, the aim of this study was to quantitatively evalu- ate the expression patterns and distribution of NKG2DL in different subpopulations of glioma stem cells, especially those showing embryonal or neural stem cell properties. In addition to in situ coexpression studies, we investigated the dynamic regulation of NKG2DL expression glioma stem- like cells in relation to differentiation status and in response to temozolomide (TMZ) treatment, a cytotoxic drug com- monly used in GBM therapy.

Materials and methods

Tissue samples and cell cultures

Human glioblastomas WHO °IV were surgically resected at the Department of Neurosurgery (Kiel, Germany). Informed consent was obtained from all individual participants included in the study. Patient's informations are given in Table 1. Median age at operation was 58 years. 40% of the patients were female. The tumor had a frontal or temporal localization in 14 cases, and a parietal or occipital localiza- tion in 8 cases (some tumors being multilocular). 19 out of 20 tumors were primary glioblastomas. 13 patients received a radiochemotherapy following the surgery (Stupp scheme: 60 Gray splitted up on 2 Gy for 5 days a week in 6 cycles plus chemotherapy with temozolomide 75 mg/m^2 body sur- face during radiation; following radiotherapy 6 cycles of TMZ 150–200 mg/m^2 body surface on 5 of 28 days). Four patients exclusively received adjuvant radiotherapy and one patient received exclusively TMZ. Two patients received no radiochemotherapy at all, due to general bad condition (Table 1). The project was in accordance with approved ethical standards of the ethics committee of the University of Kiel and the Helsinki Declaration of 1964 and its later

Table 1 Gender, age at operation, histology, localization of tumor, primary or secondary glioblastoma, and postoperative procedure of patients

No	Gender	Age	Histology	Localization	Primary/secondary	Postop procedure
1	m	56	GBM WHO °IV	Left frontal	Primary	Stupp
2	w	58	GBM WHO °IV	Right temporal	Primary	Radiotherapy
3	m	54	GBM WHO °IV	Right temporal	Primary	Stupp
4	m	75	GBM WHO °IV	Left frontal	Primary	Stupp
5	m	49	GBM WHO °IV	Left frontal	Primary	Stupp
6	w	37	GBM WHO °IV	Left temporooccipital	Secondary	TMZ
7	m	65	GBM WHO °IV	Unknown	Primary	Stupp
8	m	62	GBM WHO °IV	Right temporal	Primary	Unknown
9	w	60	GBM WHO °IV	Right temporoparietal	Primary	Stupp
10	m	54	GBM WHO °IV	Right frontal	Primary	Stupp
11	w	73	GBM WHO °IV	Right occipital	Primary	Stupp
12	w	35	GBM WHO °IV	Left parietal	Primary	Stupp
13	m	77	GBM WHO °IV	Right frontoparietal	Primary	None
14	m	65	GBM WHO °IV	Right frontal	Primary	Stupp
15	w	66	GBM WHO °IV	Right temporoparietal	Primary	Radiotherapy
16	m	42	GBM WHO °IV	Right frontal	Primary	Radiotherapy
17	m	43	GBM WHO °IV	Left frontal	Primary	Stupp
18	m	62	GBM WHO °IV	Left frontal	Primary	Stupp
19	w	64	GBM WHO °IV	Left frontal	Primary	Radiotherapy
20	w	67	GBM WHO °IV	Right occiptal	Primary	Stupp

amendments (D 405/14, D485/13, D536/15). The diagnosis was verified by a pathologist. We used commercial human glioblastoma cell lines, which were obtained from The European Collection of Authenticated Cell Cultures [ECACC, Salisbury, United Kingdom; T98G: ECACC No. 92090213; U251MG (formerly known as U373MG: ECACC No. 89081403). U251MG (formerly known as U373MG)] is named U251MG in the following. Cell cultures were routinely checked for purity by immunostaining with cell-specific markers [glial acidic fibrillary protein (GFAP); mouse, 1:500; Dako, Hamburg, Germany; and Fibronectin (H-300); rabbit, 1:100; Santa Cruz, Dallas, TX, USA] and for the absence of Mycoplasma contamination by staining with bisbenzimide as described before (Hattermann et al. 2010; Held-Feindt et al. 2010). Identity of cell lines was proven routinely by STR (Short Tandem Repeat) profiling at the Department of Forensic Medicine (Kiel, Germany) using the Powerplex HS Genotyping Kit (Promega, Madison, WC). In detail, after fluorometric quantification, DNA was amplified with an STR multiplex PCR, electrophoretic separation was performed using the 3500 Genetic Analyzer (Thermo Fisher Scientific, Waltham, MA, USA), and for evaluation, the Software GeneMapper ID-X (Thermo Fisher Scientific) was used.

Stem-like cell cultures were established by cultivating T98G and U251MG cells in neurosphere medium [50% DMEM, 50% F12 medium containing 2 mM L-glutamine (Merck Millipore, Billerica, MA, USA), 0.6% glucose (Roth, Karlsruhe, Germany), 9.5 ng/ml putrescine dihydrochloride (Sigma-Aldrich, St. Louis, MO, USA), 6.3 ng/ml progesterone (Sigma-Aldrich), 5.2 ng/ml sodium selenite (Sigma-Aldrich), 0.025 ng/ml insulin (Sigma-Aldrich), 2 µg/ml heparin (Sigma-Aldrich), and 4 mg/ml bovine serum albumin (Thermo Fisher Scientific)]. The growth factors EGF (epidermal growth factor; PeproTech, Rocky Hill, NJ, USA) and bFGF (basic fibroblast growth factor; ImmunoTools, Friesoythe, Germany) were added at a concentration of 20 ng/ml. After several passages of trypsinization processes (minimum of three, trypsinizati on every 7 days), differentiation of stem-like cells was induced by adding 10% fetal bovine serum to neurosphere medium and by removing bFGF and EGF in a subgroup of cells. After 10 days of differentiation, the corresponding stem-like cell spheres and the differentiated cells were stained by immunocytochemistry, and mRNA was analyzed by qRT-PCR as described below. Identity of stem-like and differentiated cells, respectively, was checked by analyzing the mRNA expression of glial fibrillary acidic protein (GFAP) and Sox-2 using qRT-PCR as mentioned below. In addition, stem-like cells were morphologically characterized by formation of neurospheres, which have the ability to float and which survive and proliferate under stem cell conditions. After differentiation, cells loose this ability and change their morphology to an adherent phenotype.

Quantitative RT-PCR

RNA was isolated using the Arcturus PicoPure® RNA Isolation Kit (Applied Biosystems by life technologies, Carlsbad, CA, USA) following the manufacturer's instructions for tissue or cell cultures. DNA was digested by RNase free DNase (Promega) and cDNA was synthesized by reverse transcription (Thermo Fisher Scientific). Realtime PCR was performed using TaqMan MasterMix and Primer Probes (Applied Biosystems, Waltham): human glyceraldehyd-3-phosphate dehydrogenase [*hGAPDH* (Hs99999905_m1)], *hGFAP* (Hs00157674_m1), *hOct-4* (Hs00999632_g1), *hKlf-4* (HS00358836_m1), *hSox-2* (Hs00602736_s1), *hNanog* (Hs02387400_g1), *hMusashi-1* (Hs00159291_m1), *hMICA (Hs00792195_m1), hMICB (Hs04187752_mH; alternative names DAAP-210H10.1, PERB11.2), hULBP1 (Hs00360941_m1; alternative names RAET1I, RP11-472G23.2),* and *hULBP2 (Hs00607609_mH; alternative names N2DL2, RAET1H, UNQ463/PRO791), hULBP3 (Hs00225909_m1)*. Cycle of threshold values (C_T) was measured by a cycler (QuantStudio 5, Applied Biosystems by Thermo Fisher Scientific). The genes mentioned above were normalized to the house keeping gene GAPDH yielding ΔC_T values: C_T (gene of interest)—C_T (GAPDH). As ΔC_T values mirror the exponential course of the qPCR, a ΔC_T of 3.33 corresponds to a tenfold lower expression compared to GAPDH, a ΔC_T value of 6.67 corresponds to a 100-fold lower expression, and so on. The relative gene expression compared to GAPDH ($2^{-\Delta C_T}$) was used for statistical analysis. C_T of $n = 41$, which was the maximum cycle number, was defined as undetectable. The expression differences between stem-like and differentiated cells were calculated as n-fold $\Delta\Delta C_T$ values $= 2^{\Delta C_T \text{ stem-like cells} - \Delta C_T \text{ differentiated cells}}$. After stimulation with Temozolomide, the induction of gene expression is shown as n-fold expression changes. This was calculated as $\Delta\Delta C_T$ values $= 2^{\Delta C_T \text{ control} - \Delta C_T \text{ stimulus}}$.

Immunohistochemistry

For in situ analysis of marker expression, 10 µm cryosections of 20 different glioma patients were stained by immunohistochemistry. Fixation was performed with an ice-cold acetone–methanol mixture (1:1) for 10 min; blockage for autofluorescence was obtained with sudan black (1% in 70% ethanol, Roth). Afterwards, blockage for unspecific antibody binding was performed by adding 0.5% glycine/0.5% bovine serum albumin. Primary antibodies were added and incubated over night at 4 °C. Secondary antibodies were incubated at 37 °C for 1 h. Nuclei were stained with diamidino-2-phenylindol (DAPI; Sigma–Aldrich; 1:30,000) which was applied at room temperature for 30 min. All antibodies were diluted in phosphate-buffered saline (PBS) for cell cultures and tris-buffered saline with 0.1% Tween (TBST)

for cryo-sections. Sections were embedded with Immumount (Thermo Fisher Scientific). After each step, slides were washed with TBST. Primary antibodies were anti-GFAP (mouse, 1:500; Dako), anti-OCT4 (rabbit, 1:150; Cell Signaling, Danvers, MA, USA), anti-KLF4 (1:250, mouse; Thermo Fisher Scientific), anti-SOX2 (rabbit, 1:200; Santa Cruz), anti-Nanog (rabbit, 1:500,; Thermo Fisher Scientific), anti-Musashi-1 (mouse, 1:100,; R&D Systems, Minneapolis, MN, USA), anti-MICA 2C10 (mouse, 1:150; Santa Cruz), anti-MICB (mouse, 1:500, R&D Systems), anti-ULBP1 (rabbit, 1:200, proteintech, Chicago, IL, USA), anti-ULBP2 (rabbit, 1:500, abcam, Cambridge, UK), anti-ULBP3 (mouse, 1:250, R&D), anti-CD3γ (rabbit, 1:200, Thermo Fisher Scientific), anti-von Willebrand factor (vWF) (mouse, 1:1000, Santa Cruz), and anti-cluster of differentiation (CD)11b (mouse, 1:100, Santa Cruz). When both primary antibodies were derived from the same species, unspecific binding was blocked by adding F(ab) fragments from the very same species (donkey anti-mouse and anti-rabbit F(ab) fragments, 1:1000, from Jackson ImmunoResearch, West Grove, PA, USA). This step was left out when both primary antibodies were derived from different species. Afterwards, secondary antibodies were added. Isotype controls were performed by applying IgG$_1$ mouse and IgG$_1$ rabbit (both R&D Systems) in concentration adapted to the other primary antibodies used. As secondary antibodies, donkey anti-mouse or anti-rabbit IgGs labelled with Alexa Fluor 488 or Alexa Fluor 555 (1:1000; Invitrogen, Carlsbad, CA, USA) were used. For negative controls, primary antibodies were omitted exclusively. Manufacturers of all antibodies provided proof of validation of technical specifity. To allow a better structural analysis, hematoxylin and eosin (H&E) stainings were performed on all examined tumors according to standard protocols.

Quantitative analysis

To evaluate relative proportions of cells being positive for various NKG2DL and stem cell markers, we performed a quantitative analysis of stained cryosections of 20 different glioma patients. For this purpose, the number of cells positive for the respective marker, the number of cells being positive for both markers, and the absolute cell count were surveyed manually in five different fields of view of a microscope for every section. Afterwards, the mean values and the standard deviations were calculated.

Immunocytochemistry

For in vitro analysis of stem cell markers and NKG2DL expression, stem-like spheres and the corresponding differentiated cells derived from the glioma cell lines T98G and U251MG were seeded on cover glasses and were stained

as described above. After fixation with ice-cold methanol–acetone (1:1 mixture), cells were washed with PBS. All other steps were performed as mentioned in the description of immunohistochemistry, including isotype and negative controls.

Microscopy

Images were obtained with a Zeiss Oberver.Z1 microscope (Zeiss, Oberkochen, Germany). Plan-Apochromat 40x/1.4 Oil DIC (CN) VIS-IR M27 was used as a lens. The camera AxioCam MR MR5 (Zeiss) with a focus depth of 0.89 µm for 555 nm, 0.80 µm for 488 nm, and 0.72 µm for DAPI was used. For image processing, ZEN2 (blue edition, 2011) was used (Zeiss). Images had a size of 1388×1040 pixels ($223,82 \times 167,70$ µm) at an image bit depth of 12 bit.

Stimulation experiments

For stimulation experiments, T98G and U251MG GBM cells were seeded subconfluently on 6-well plates and were cultivated for 24 h. Cultures were kept in neurosphere medium with temozolomide (Sigma-Aldrich, 500 µM) or corresponding concentrations of DMSO as solvent control. Cells were incubated for 48 h. Afterwards, RNA was isolated using the Arcturus PicoPure® RNA Isolation Kit (Applied Biosystems by Life Technologies).

Statistical analysis

Mean value and standard deviation were calculated. For testing significance of increase or decrease of expression, Student's t test was used (2-sided, paired test). Undetectable samples were set at $C_T = 41$, as this would commonly represent the detection limit if 40 amplification cycles are run. P values were indicated in the following way: $* < 0.05$, $** < 0.01$, and $*** < 0.001$.

Results

In situ expression and localization of NKG2DL in human glioblastomas

To evaluate the in situ distribution and localization of NKG2DL, we stained cryo-sections of primary human glioblastomas for the NKG2DL MICA, MICB, ULBP1, 2, and 3 in combination with each other, in combination with glial fibrillary acidic protein (GFAP), cluster of differentiation 3 gamma chain (CD3γ), cluster of differentiation 11b (CD11b), and von Willebrand factor (vWF) and in combination with various stem cell markers (Klf-4, Oct-4, Sox-2, Nanog, and Musashi-1).

Double-immunostaining of NKG2DL with each other and in combination with GFAP, CD3γ, CD11b, and vWF

To initially identify NKG2DL-positive cell subsets within the tumors per se and to evaluate their relationship to stromal or infiltrating immune cells, we performed double-immunostaining of various NKG2DL (MICA, MICB, ULBP1, 2, and 3) with each other, with GFAP, CD3γ, CD11b, and vWF. Here, NKG2DL-positive cells were only rarely found in clusters, but were mostly scattered and rarely directly neighbored to each other. Moreover, with exceptions of the combination of MICB with ULBP2, we observed a broad costaining of all NKG2DL with each other (exemplary sections in Fig. 1, first column). Isotype controls were performed for every possible combination of mouse or rabbit primary and secondary antibodies (exemplary results shown in Fig. 2). NKG2DL-positive cells were found in GFAP-positive tumor regions (Fig. 1, second column), and sometimes a costaining of every single NKG2DL with CD3γ, a common cluster of differentiation found on T cells (Fig. 1), was seen as well. However, there were also single-positive cells for CD3γ and MICA, MICB, ULBP1, 2, and 3, respectively (Fig. 1). We also observed that CD3γ-positive cells often appeared in clusters, whereas NKG2DL-positive cells were mostly scattered and isolated. It was shown that glioblastoma-infiltrating antigen-presenting cells, consisting mainly of microphages/microglia, can also express NKG2DL (Kmiecik et al. 2013), Here, when analyzing double-immunostaining for CD11b, a cluster of differentiation found on macrophages and microglia and being involved in numerous adhesion–related associations, we observed a costaining with NKG2DL only very rarely (Fig. 1). Looking at the double-immunostaining of NKG2DL and vWF, which usually is found in vessel endothelium and can be released into the plasma and the basement membrane of endothelial cells, NKG2DL-positive cells were found in the penumbra of tumor vessels, but were not costained (Fig. 1). CD3γ and vWF also were not found to be costained (Fig. 1, bottom of first column). Negative controls and isotype controls are summarized in Fig. 2.

Double-immunostaining of NKG2DL with various stem cell markers

To further evaluate the in situ distribution of NKG2DL in regard to stem cells within the tumor, we performed double-immunostaining of MICA, MICB, ULBP1, 2, and 3 in combination with the stem cell markers Klf-4, Oct-4, Sox-2, Nanog, and Musashi-1, which are all neural/embryonal stem cell markers well documented in gliomas, and analyzed the results quantitatively. (Fluh et al. 2016; Hattermann et al. 2016). Representative results for double-immunostaining are shown in Fig. 3. Again, NKG2DL were found only in a
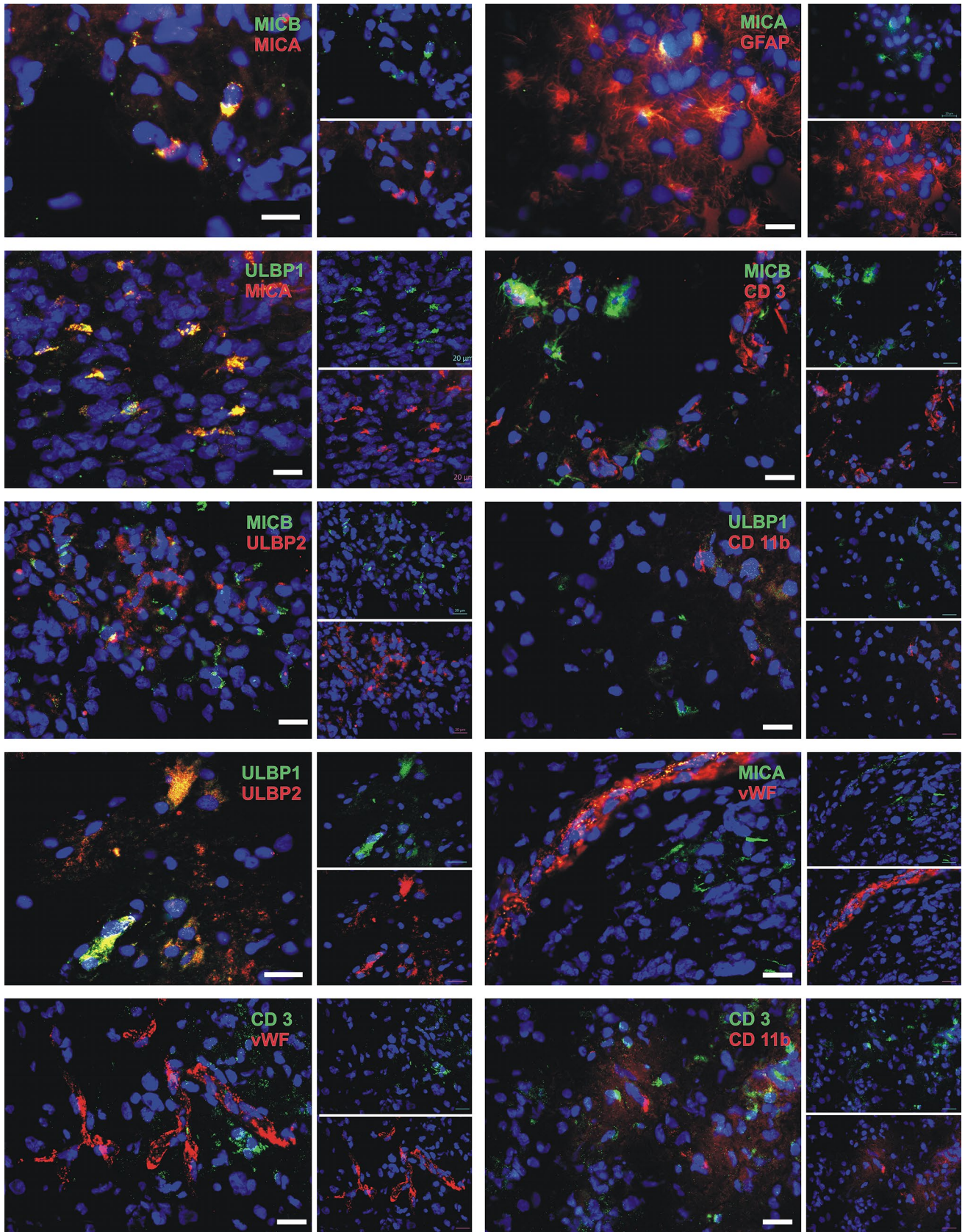
◀**Fig. 1** Double-immunostaining of NKG2DL with each other and in combination with GFAP, CD3γ, CD11b, and vWF. Selected images from different primary human GBM; Costaining of MICA with MICB, MICA with ULBP1, MICA with ULBP2, MICB with ULBP1, and ULBP1 with ULBP2 was found frequently, and we found partial costaining of MICB with ULBP2. NKG2DL-positive cells were found in GFAP-positive tumor regions. Costaining of NKG2DL (green) with CD3γ (red) was found, as well, although single-positive cells for both markers were found, respectively. There was almost no/rare costaining of NKG2DL with CD11b; NKG2DL were found in the penumbra of vWF-positive regions, but were not costained with vWF. Bars are indicating 20 µm

distinct tumor cell subpopulation and these NKG2DL positive cells were not found in clusters. As we observed in a previous study (Hattermann et al. 2016), only a small subpopulation of tumor cells showed positive staining of the respective stem cell markers, and these cells were commonly found in small clusters. This applied to all of the examined stem cell markers (Figs. 2, 3). Notably, HE staining revealed that all examined GBMs resembled typical characteristics for highly malignant, actively proliferating tumors. We frequently found mitosis, neovascularization, and necrotic areas (exemplarily depicted in Fig. 4).

Initially, we performed a quantitative analysis on 20 different GBM samples according to individual NKG2DL and stem cell markers' positive cell amounts. Here, MICA was found in 5% [standard deviation (SD) ± 2%], MICB in 4% (SD ± 2%) ULBP1 in 14% (SD ± 3%), ULBP2 in 3% (SD ± 1%), and ULBP3 in 5% (SD ± 1%) of the tumor cells. Whereas Musashi-1 was found in only 2% of all tumor cells (SD ± 2%), all other stem cell markers were found at a similar frequency [14% (SD ± 11%) were positive for Oct-4, 14% (SD ± 6%) for Klf-4, 12% (SD ± 1%) for Sox-2, and 16% (SD ± 2%) for Nanog].

Next, we analyzed the amount of NKG2DL-positive cells being costained for various stem cell markers. For Klf-4, a transcription factor and a classical marker for embryonic stem cells (Bradshaw et al. 2016), we observed a frequent costaining with MICA [94% (SD ± 24%) positive for Klf-4], MICB [82% (SD ± 23%) positive for Klf-4], ULBP1 [93% (SD ± 12%) positive for Klf-4], ULBP2 [84% (SD ± 23%) positive for Klf-4] and ULBP3 [89% (SD ± 18%) positive for Klf-4]; exemplary sections, as shown in Fig. 3. Looking at Oct-4, we observed a costaining with MICA [37% (SD ± 42%) of cells, positive] and MICB [21% (SD ± 32%) of cells, positive] in relatively low amounts (Fig. 2), whereas ULBP1 (89%, SD ± 34%) was frequently costained, and ULBP2 (59%, SD ± 36%) and ULBP3 (61%, SD ± 42%) were found to be costained at an intermediate level (Fig. 3). Concerning Sox-2, we found an intermediate costaining with MICA (74%, SD ± 31%), MICB (75%, SD ± 26%), ULBP2 (59%, SD ± 38%), and ULBP3 (65%, SD ± 25%), and a frequent costaining with ULBP2 (97%, SD ± 8%). Similar results were found for Nanog, which was found in

67% (SD ± 25%) of MICA-positive cells, 67% (SD ± 32%) of MICB-positive cells, 69% (SD ± 48%) of ULBP2-positive cells, but 97% (SD ± 7%) of ULBP1-positive cells and 92% (SD ± 12%) of ULBP3-positive cells (Fig. 3). Musashi-1 was found to be costained with any of the NKG2DL in ligand-dependent different but overall at relatively low amounts [26% (SD ± 36%) in MICA, 36% (SD ± 37%) in MICB, 20% (SD ± 23%) in ULBP1, 0% in ULBP2, 4% (SD ± 13%) in ULBP3; Fig. 3]. Results are shown in Table 2. Again, corresponding negative and isotype controls are summarized in Fig. 2.

Vice versa, as compared to all other investigated NKG2DL, ULBP1 was expressed in cells with stem cell characteristics at the highest percentages [89% (SD ± 34%) of Oct-4-positive cells, 76% (SD ± 30%) of Klf-4-positive cells, 88% (SD ± 21%) of Sox-2-positive cells, 71% (SD ± 30%) of Nanog-positive cells, and 57% (SD ± 36%) of Musashi-1-positive cells]. MICA was found at moderate-to-low levels (22% (SD ± 27%) in Oct-4-positive cells, 43% (SD ± 29%) in Klf-4, 35% (SD ± 30%) in Sox-2, 33% (SD ± 21%) in Nanog, and 47% (SD ± 45%) in Musashi-1-positive cells). MICB was found in low amounts in Oct-4 (9%, SD ± 14%), Sox-2 (25%, SD ± 23%), Nanog (27%, SD ± 27%) and Musashi-1 (20%, SD ± 35%) positive cells but frequently found in Klf-4 positive cells (76%, SD ± 31%). ULBP2 was, compared to other NKG2DL, found at relatively low percentages [21% (SD ± 30%) of Oct-4, 12% (SD ± 16%) of Klf-4, 14% (SD ± 19%) of Sox-2, 15% (SD ± 21%) of Nanog-, and 0% of Musashi-1-positive cells]. ULBP3 was found at moderate levels in stem cell-maker positive cells [21% (SD ± 22%) in Oct-4, 48% (SD ± 33%) in Klf-4, 43% (SD ± 35%) in Sox-2 and in 38% (SD ± 28%) of Nanog-positive cells]. Musashi-1-positive cells showed costaining with ULBP3 in 100%. This effect might be aggravated due to the relatively low number of Musashi-1-positive cells per tumor. Results are shown in detail in Table 3.

Summarized, the distribution of NKG2DL on stem cell marker positive cells in human glioblastomas is heterogeneous. Importantly, many NKG2DL-positive cells seem to be positive for Klf-4 and to a lesser extent for Sox-2 and Nanog. Musashi-1 is rarely found in NKG2DL-positive cells. Only few cells positive for MICA and MICB showed staining for Oct-4. However, not all NKG2DL-positive cells express stem cell markers and *vice versa*.

In vitro expression of NKG2DL and stem cell markers in stem-like cells and corresponding differentiated cells derived from different glioma cell lines

To analyze whether the specific distribution of NKG2DL described above and stem cell marker expression was reproducible in vitro, we examined glioma stem-like spheroids derived from exemplary glioma cell lines T98G und

Fig. 2 Negative and isotype controls for all used antibodies. Negative controls for GBM cryosections (**a**) and cell cultures (stem cells and corresponding differentiated cells **b**) are shown in the first column. Mouse and rabbit AF 488 and AF 555 were used, respectively. Isotype controls for GBM cryosections (**a**) and cell cultures (stem cells and corresponding differentiated cells **b**) are shown in the second column. Here, mouse and rabbit IgG labelled with either AF 488 or AF 555 were used
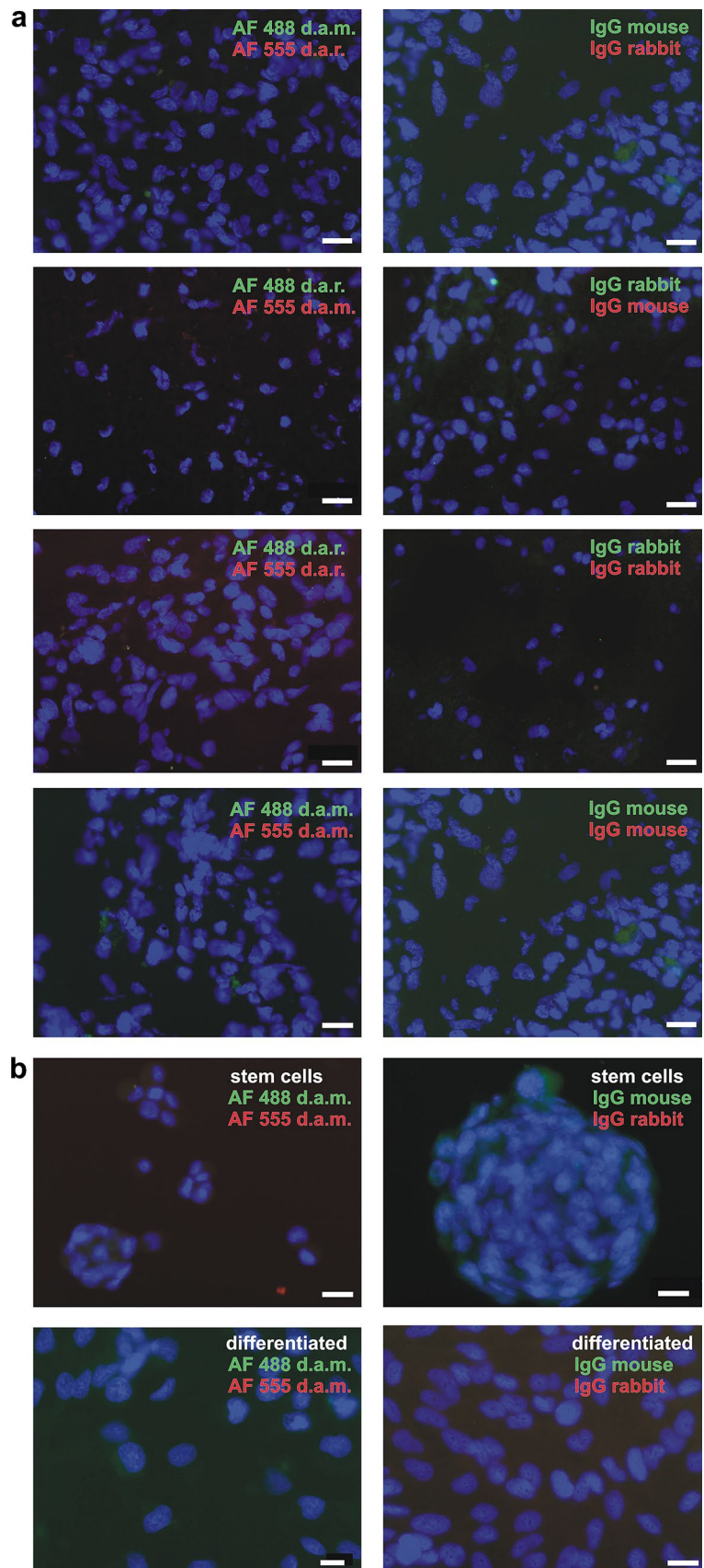
Fig. 3 Double immunostaining of NKG2DL with the neural/embryonal stem cell markers Klf-4, Oct-4, Sox-2, Nanog, and Musashi-1. Selected images from different primary human GBM; here, we show MICA with Oct-4 (only 22% of Oct-4-positive cells were positive for MICA; 37% of MICA-positive cells were positive for Oct-4), MICB with Sox-2 (25% of Sox-2-positive cells were positive for MICB; 75% of MICB-positive cells were positive for Sox-2), ULBP1 with Musashi-1 (57% of Musashi-1-positive cells were positive for ULBP1; 20% of ULBP1-positive cells were positive for Musashi-1), ULBP2 with Nanog (15% of Nanog-positive cells were positive for ULBP2; 69% of ULBP2-positive cells were Nanog-positive) and ULBP3 with Klf-4 (48% of Klf-4-positive cells were ULBP3-positive; 89% of ULBP3-positive cells were Klf-4-positve). Bars are indicating 20 μm

U251MG by cultivation in neurosphere medium and corresponding differentiated cells generated from these spheroids. Differentiation of the spheres was induced by adding 10% FBS to the neurosphere medium and omitting the growth factors bFGF and EGF as described before (Hattermann et al. 2010). In neurosphere medium, the cultures showed the typical free floating spheroid morphology of stem-like cells. After adding 10% FBS, cell morphology changed into an adherent, more differentiated phenotype. We analyzed expression changes comparing stem-like cells with differentiated cells on mRNA level by qRT-PCR and on protein level by immunocytochemistry.

Remarkably, MICA and ULBP2 were expressed at a significantly higher baseline level in U251MG compared to T98G, while MICB and ULBP1 were significantly higher expressed in T98G compared to U251MG. Furthermore, qRT-PCR revealed that MICB was expressed significantly higher in stem-like cells derived from T98G compared to the corresponding differentiated cells. Higher expression in T98G stem-like cells compared to differentiated cells was seen for MICA und ULBP2 as well, but was missing significance in both markers. Concerning ULBP3-expression, no significant differences were seen between T98G and U251MG. Looking at U251MG, we did not observed any significant change in expression of NKG2DL when comparing stem-like cells with differentiated cells (Fig. 5a). Regarding the expression of stem cell markers, most markers were—as expected—expressed at a higher level in stem-like cells. This effect was more pronounced in U251MG. Here, we saw a highly significant higher expression of Sox-2 and Nanog in spheroids compared to differentiated cells (Fig. 5b). This effect was also seen concerning Klf-4 and Musashi-1. When looking at spheroids and differentiated cells derived from T98G, we saw a moderate, but not significantly higher expression of Klf-4, Oct-4, and Nanog in spheroids compared to differentiated cells (Fig. 5b). Interestingly, Sox-2 and Nanog were expressed at a significantly higher baseline level in U251MG compared to T98G. This effect was seen for Musashi-1 as well, although not significant in this case. The mRNA expression results of NKG2DL
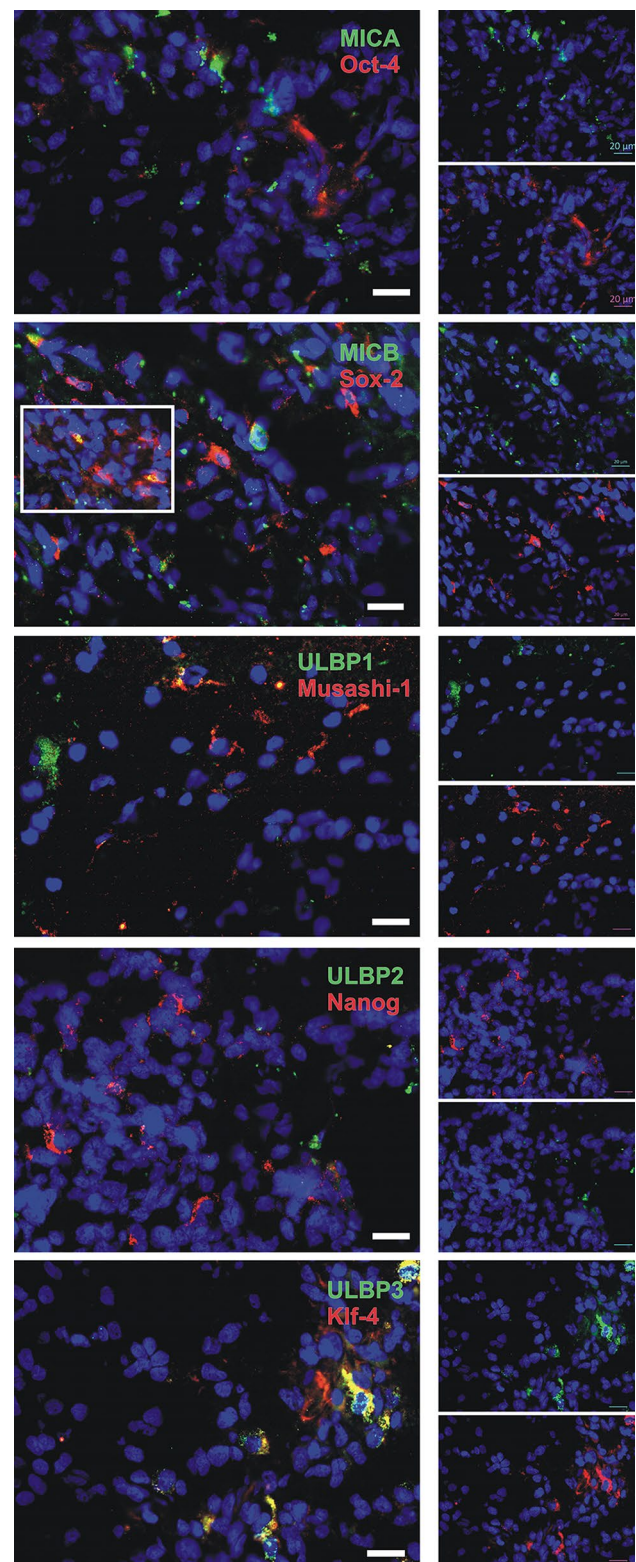
and stem cell markers obtained by qRT-PCR were confirmed on protein level by immunostainings, as exemplarily shown in Fig. 5c. Isotype and negative controls were perfomed for mouse and rabbit primary antibodies, using either mouse or
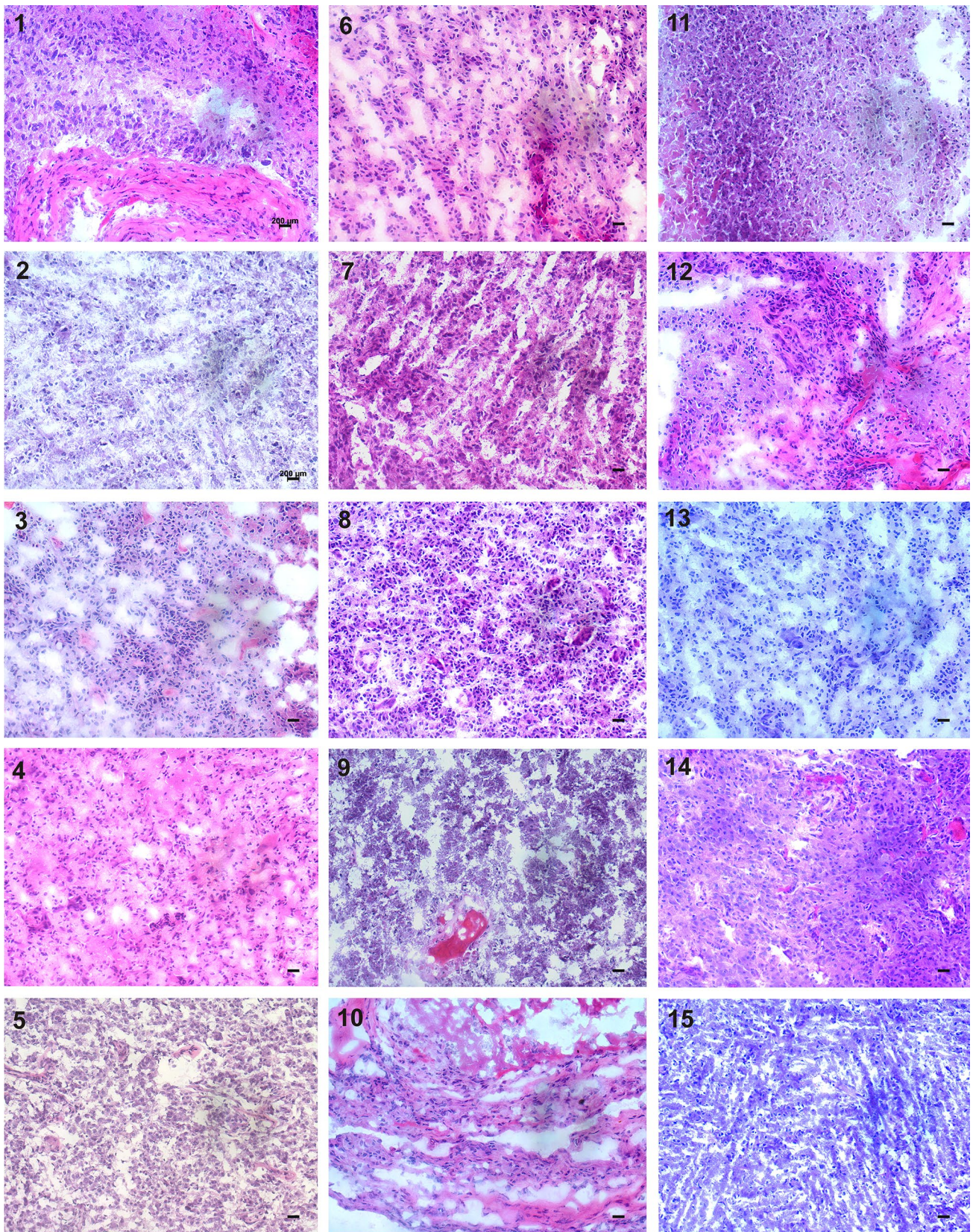
Fig. 4 Selected HE staining of 15 out of 20 glioblastoma. All tumors resemble typical histological features like mitoses, neovascularization, and necrosis

Table 2 Amount of NKG2DL-positive cells being costained for various stem cell markers

	Klf-4	Oct-4	Sox-2	Nanog	Musashi-1
MICA	94% (SD ± 24%)	37% (SD ± 42%)	74% (SD ± 31%)	67% (SD ± 25%)	26% (SD ± 36%)
MICB	82% (SD ± 23%)	21% (SD ± 32%)	75% (SD ± 26%)	67% (SD ± 32%)	36% (SD ± 37%)
ULBP1	93% (SD ± 12%)	89% (SD ± 34%)	97% (SD ± 8%)	97% (SD ± 7%)	20% (SD ± 23%)
ULBP2	84% (SD ± 23%)	59% (SD ± 36%)	59% (SD ± 38%)	69% (SD ± 48%)	0%
ULBP3	89% (SD ± 18%)	61% (SD ± 42%)	65% (SD ± 25%)	92% (SD ± 12%)	4% (SD ± 13%)

Table 3 Amount of stem cell marker positive cells being costained for various NKG2DL

	MICA	MICB	ULBP1	ULBP2	ULBP3
Klf-4	43% (SD ± 29%)	76% (SD ± 31%)	76% (SD ± 30%)	12% (SD ± 16%)	48% (SD ± 33%)
Oct-4	22% (SD ± 27%)	9% (SD ± 14%)	89% (SD ± 34%)	21% (SD ± 30%)	21% (SD ± 22%)
Sox-2	35% (SD ± 30%)	25% (SD ± 23%)	88% (SD ± 21%)	14% (SD ± 19%)	43% (SD ± 35%)
Nanog	33% (SD ± 21%)	27% (SD ± 27%)	71% (SD ± 30%)	15% (SD ± 21%)	38% (SD ± 28%)
Musashi-1	47% (SD ± 45%)	20% (SD ± 35%)	57% (SD ± 27%)	0%	100%

rabbit IgG or omitting all primary antibodies and using PBS instead (Fig. 2).

The overall picture is summarized in Fig. 5d as a diagram. Starting off with a distinct baseline expression profile of NKG2DL and stem cell markers, which differed between T98G and U251MG spheroids, spheroids derived from U251MG showed more plasticity of stem cell marker expression upon differentiation than spheroids derived from T98G. Contrasting this, NKG2DL expression changes in T98G spheroids upon differentiation were more pronounced. Summarized, it seemed that a specific distribution of NKG2DL and stem cell marker expression exists both in solid glioblastoma samples in situ and cultured glioma spheroids in vitro. Here, spheroids from U251MG and T98G closely mirrored different population of NKG2DL and stem cell marker expressing glioma cells, showing different regulation patterns upon differentiation.

### In vitro regulation of NKG2DL by temozolomide in stem-like cells derived from glioma cell lines

To evaluate the influence of temozolomide (TMZ), the most common chemotherapeutic agent used in standard GBM treatment, on mRNA expression levels of MICA, MICB, ULBP1, and 2 in glioma stem-like cells in vitro, we stimulated spheroids derived from the glioma cell lines T98G and U251MG with 500 μM of TMZ for 48 h ($n = 3$). As TMZ was dissolved in DMSO, equal amounts of DMSO were added for controls, which were used to determine the n-fold induction of mRNA expression (n-fold expression for DMSO control = 1; results shown in Fig. 6). We detected a significant induction of all NKG2DL after stimulation with TMZ in spheroids derived from T98G (left part of Fig. 6). Here, detailed n-fold induction values were 2.87 ± 0.83 for MICA, 2.19 ± 0.31 for MICB, 3.15 ± 0.77 for ULBP1,

and 3.36 ± 1.48 for ULBP2. Concerning spheroids derived from U251MG, we saw a significant upregulation of MICA, MICB, and ULBP2 (right part of Fig. 6). As already seen in unstimulated spheroids derived from U251MG, ULBP1 was not detectable (n.d.). Detailed n-fold induction values were 1.95 ± 0.39 for MICA, 4.35 ± 0.85 for MICB, and 2.39 ± 0.17 for ULBP2.

Thus, TMZ stimulation significantly induced the expression of NKG2DL in stem-like spheroids generated from T98G and U251MG cell lines.

Discussion

Compared to many other tumors, prognosis of patients with GBM is, with a median survival of 14 months, poor (Stupp et al. 2009). Mechanisms of escape to the current standard therapeutic strategies involve tumor heterogeneity, immunological escape mechanisms including the NKG2D system, and therapy resistance of tumor cells, especially with stemness features. Tumor stem cells are, according to the stem cell hypothesis, a subpopulation of tumor cells with the ability of unlimited self-renewal and asymmetric division and have been described to be the source of recurrence and metastases in many tumors (Ignatova et al. 2002; Al-Hajj et al. 2003; Barker et al. 2009; O'Connor et al. 2014; Hattermann et al. 2016). The NKG2D system itself is a mechanism of immunologic defense, which plays an important role in recognition and elimination of tumor cells (Nausch and Cerwenka 2008). Although others showed that stem-like cells derived from commercial glioma cell lines and primary human glioblastoma expressed NKG2DL on their surface (Di Tomaso et al. 2010; Wolpert et al. 2014), detailed information on the specific distribution of NKG2DL in different subpopulations of glioma stem cells does not yet exist. Here,
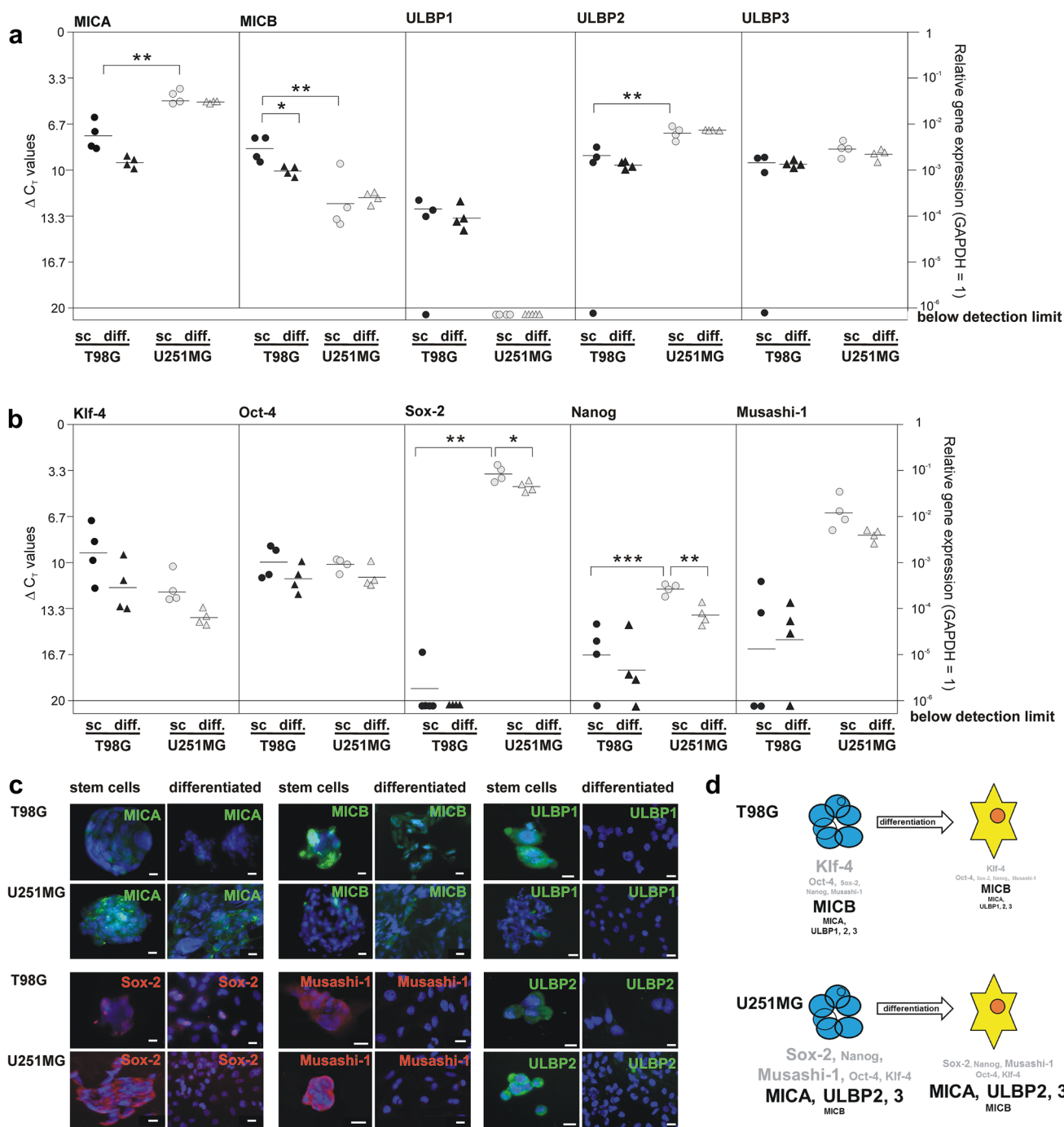
we aimed at characterizing the quantitative distribution pattern of NKG2DL (MICA, MICB, ULBP1, and ULBP2) on glioma stem cells in situ and in vitro. In both approaches, we distinguished different subpopulations of glioma stem cells by the expression of different neural and embryonal stem cell markers (Oct-4, Sox-2, Nanog, Musashi-1, and Klf-4) and additionally analyzed the effect of Temozolomide on NKG2DL expression in glioma stem-like cells in vitro.

In contrast to some other studies, which found NKG2DL to be only rarely detectable by staining of human glioblastoma sections (Di Tomaso et al. 2010), we found NKG2DL to be present in all glioblastomas at a well-detectable level. However, it seems that only a subset of glioma cells express NKG2DL. These cells were located in GFAP-positive regions, and a part of them were double-positive for NKG2DL and specific stem cell markers in individual NKG2DL and stem cell marker-specific amounts. As the surface expression of NKG2DL correlates with the probability of the expressing cell to be identified by NK or T cells, which usually leads to induction of apoptosis, the

◄**Fig. 5** In vitro expression of NKG2DL (MICA, MICB, ULBP1, ULBP2, and ULBP3) and stem cell markers (Klf-4, Oct-4, Sox-2, Nanog, and Musashi-1) in stem-like cells and corresponding differentiated cells derived from the glioma cell lines T98G and U251MG. We analyzed mRNA level by qRT-PCR (**a** and **b**) and protein level by immunocytochemistry (**b**). Baseline expression level of MICA and ULBP2 was higher in U251MG, whereas baseline expression levels of MICB and ULBP1 was higher in T98G (**a**). Baseline level of ULBP3 was similar in T98G and U251MG (**a**). Baseline expression of Sox-2, Nanog and Musashi-1 was higher in U251MG stem-like cells compared to T98G stem-like cells (**b**). qRT-PCR of stem-like spheres in comparison to corresponding differentiated cells revealed that T98G stem-like cells expressed MICA, MICB, and ULBP2 at a significantly higher level than differentiated cells; no such difference was seen in U251MG (**a**). Expression of Klf-4, Sox-2, Nanog, and Musashi-1 decreased with differentiation; this effect was more pronounced in U251MG than in T98G. ΔCT values indicate the relative gene expression in comparison to the house keeping gene GAPDH in a logarithmic plotting (left axis), which means that a 3.33 lower ΔC_T value denotes a tenfold lower gene expression (depicted in a logarithmic scale on the right axis). If the C_T value of one fraction was below the detection limit after 40 PCR cycles, this was marked as "below detection limit". A two-tailed paired Student's *t* test was used for statistical analysis. Stars indicate the following significance levels: ***$p \leq 0.001$; **$p \leq 0.01$; *$p \leq 0.05$. Results on mRNA level were confirmed on protein level by immunostaining of spheroids compared to differentiated cells; NKG2DL are shown in green; staining for Sox-2 and Musashi-1 are shown in red as examples for stem cell markers (**c**). Corresponding to our findings on mRNA levels, protein expression of NKG2DL and stem cell markers were distinctly decreased upon differentiation. The overall picture is summarized in Fig. 3d; stem cell markers are shown in light gray; NKG2DL are shown in black; stem-like cells/spheroids are shown in blue; and differentiated cells are shown in yellow (**d**)

heterogeneity of glioma stem cells concerning the NKG2DL expression in situ might be an important factor concerning the survival of tumor stem cells. Heterogeneity concerning NKG2DL expression has been described for many other non-CNS tumors (Pende et al. 2002; Vetter et al. 2002; Friese et al. 2003; Salih et al. 2003; Watson et al. 2006; Carlsten et al. 2007; Castriconi et al. 2007). Following our results, this variability also exists in glioma stem cells on a cellular level within each tumor.

We also observed a partial costaining of all examined NKG2DL and CD3γ, a common cluster of differentiation found on T cells, as well as a broad costaining of nearly all examined NKG2DL with each other. Although NKG2DL are known to be found on tumor cells or other cells under different conditions of cellular stress, T cells activated by antigen-presenting cells and T-cell blasts stimulated with super antigens (anti-CD3/anti-CD28 in combination with PMA) are known to upregulate NKG2DL (Molinero et al. 2002; Nausch and Cerwenka 2008). Moreover, Nakamura et al. reported that NKG2DL were also found on NK cells (Nakamura et al. 2013). However, in our staining experiments with glioblastoma frozen sections, the majority of NKG2DL-positive cells were CD3γ-negative. In addition, we observed only a very rare costaining with CD11b, which

is a typical marker for resident microglia, as the resident macrophage-like antigen-presenting cell of the central nervous system. Resting microglia were shown to express NKG2DLs at high levels yet in in vitro cell culture settings, activated tumor microglia in contrast express NKG2DL only at very low levels in both in vitro and in vivo experimental conditions, thus protected from NKG2D-dependent recognition and elimination. (Lunemann et al. 2008; Pereboeva et al. 2015). We also could show that the NKG2DL-positive cells seem to be located outside of tumor vessels.

In contrast to Di Tomaso et al., who found NKG2DL only very rarely expressed in glioma stem-like cells and corresponding differentiated cells, we were able to show heterogeneous but mostly distinct expression patterns of NKG2DLs in T98G and U251MG glioma stem-like cells. Interestingly, upon differentiation, mRNA expression of MICB decreased in T98G but not in U251MG. In line with our findings, Di Tomaso et al. found a heterogeneous expression of various NKG2DL in stem-like cells and corresponding differentiated cells, and—concerning U251MG—there was no clear change in NKG2DL expression upon differentiation (Di Tomaso et al. 2010). In another study, higher NKG2DL expression levels were reported on glioma long-term cell lines compared to glioma-initiating cell lines, in our system resembling more differentiated and stem-like cells, respectively (Codo et al. 2014). Interestingly, Friese et al. described that constitutive NKG2DL expression in differentiated glioblastoma cells is too low to promote an effective immune cell activation in vivo (Friese et al. 2003). As we observed a higher (T98G) or equal (U251MG) NKG2DL expression on glioma stem-like cells in comparison to corresponding differentiated cells, there might be crucial differences between differentiated cells and stem cells concerning their immunogenicity. Mechanisms leading to such heterogeneity are not entirely clear. For instance, Wolpert et al. found that there is only a partial overlap between NKG2DL surface expression and expression on mRNA level (Wolpert et al. 2014), giving a hint to additional mechanisms of posttranslational and posttranscriptional regulation (Raulet et al. 2013). As a potential mechanism of viral immune escape, human cytomegalovirus was shown to induce a loss of surface MICB by interrupting maturation and transition of MICB via the secretory pathway (Wu et al. 2003; Spreu et al. 2006).

Concerning the influence of chemotherapeutic treatment on NKG2DL expression especially in glioma stem-like cells, we saw a significant upregulation of all expressed NKG2DL. These results are in accordance with others concerning the influence of TMZ on NKG2DL expression in differentiated glioma cells (Lamb et al. 2013; Chitadze et al. 2017). In a previous study, we also could show that the increase of NKG2DL surface expression in differentiated glioma cells after stimulation with TMZ leads to a sensitization of GBM cells to γδ T cell-mediated lysis, which involves both the
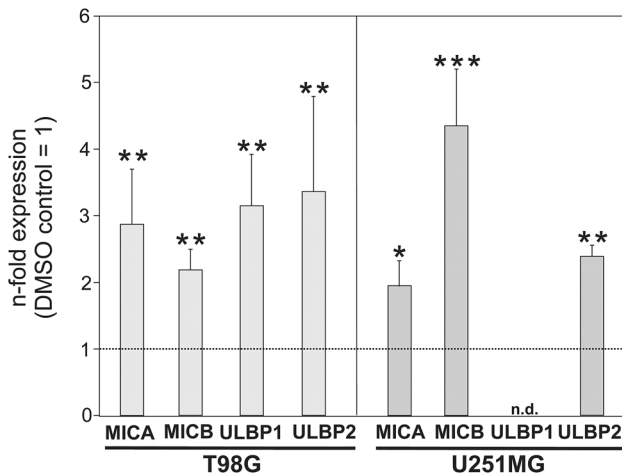
Fig. 6 Stimulation of stem-like cells derived from the glioma cell lines T98G and U251MG with TMZ (500 μM, 48 h). Induction is shown as *n*-fold expression in comparison to the solvent control treated with equal volumes of DMSO. The relative mRNA expression change of stimulated spheroids in comparison to their corresponding unstimulated spheroids was calculated as *n*-fold regulation treated/untreated $=2^{\Delta C_T\,\text{unstimulated}-\Delta C_T\,\text{stimulated}}$. Stimulations were performed in $n=3$ independent experiments. If the C_T value of one fraction was below the detection limit after 41 PCR cycles, the relative expression was calculated using this detection limit. In case of being undetectable, this was marked as "n.d." (not detectable). A two-tailed paired Student's *t* test was used for statistical analysis. Stars are indicating the following: ***$p \le 0.001$; **$p \le 0.01$; *$p \le 0.05$. TMZ led to a significant induction of all NKG2DL in spheroids derived from T98G (left part). Concerning spheroids derived from U251MG, we observed a significant upregulation of MICA, MICB, and ULBP2 (right part). As already seen in unstimulated spheroids derived from U251MG, ULBP1 was not detectable (n.d.)

NKG2D-receptor and the T-cell receptor (Chitadze et al. 2017) and could result in enhanced elimination of the tumor cell. On the other hand, an elevation of NKG2DL surface expression might lead to enhanced shedding of the ligands, which results in reduction of ligand density on the tumor cell surface, downregulation of NKG2D receptor density on effector cells, and blockage of the NKG2DR-binding site for surface expressed NKG2DL. Possibly, these mechanisms are also relevant for TMZ-upregulated NKG2DL expression in glioma stem-like cells, contributing to more anti- or pro-tumorigenic properties of upregulated NKG2DL in these special glioma subpopulations. However, it has to be taken into account that several agents used in classical chemotherapies or radiotherapies cause DNA damage, which is one of the pathways of induction of NKG2DL (Gasser et al. 2005). It has to be evaluated, if this is the only reason for the induction of NKG2DL expression after stimulation with TMZ or if there might exist a more specific pathway. TMZ-induced upregulation of NKG2DL following a chemotherapy with TMZ in GBM might be of high clinical importance, since

patients might respond differently to yet experimental immunotherapies.

In summary, the role of NKG2DL in glioma stem cells is complex. In solid glioblastomas, NKG2DL are found in a subset of tumor cells that coexpress some but not all of the investigated embryonic and neural stem cell markers, whereas stem cell like cells derived from glioma cell lines express NKG2DL and show a heterogeneous picture concerning NKG2DL and stem cell marker expression, depending on the cell line. Stimulation with TMZ leads to an upregulation NKG2DL in generated glioma stem-like cells. All in all, as stem cell like cells derived from glioma cell lines tend to show a higher expression of NKG2DL than differentiated tumor cells in vitro, the NKG2D system might play an important role in regulation of tumor stem cell survival.

Compliance with ethical standards

Conflict of interest There are no conflicts of interest.

References

Al-Hajj M, Wicha MS et al (2003) Prospective identification of tumorigenic breast cancer cells. Proc Natl Acad Sci USA 100(7):3983–3988

Aum DJ, Kim DH et al (2014) Molecular and cellular heterogeneity: the hallmark of glioblastoma. Neurosurg Focus 37(6):E11

Bao S, Wu Q et al (2006) "Glioma stem cells promote radioresistance by preferential activation of the DNA damage response. Nature 444(7120):756–760

Barker N, Ridgway RA et al (2009) Crypt stem cells as the cells-of-origin of intestinal cancer. Nature 457(7229):608–611

Bassoy EY, Chiusolo V et al (2016) Glioma stemlike cells enhance the killing of glioma differentiated cells by cytotoxic lymphocytes. PLoS One 11(4):e0153433

Beier CP, Kumar P et al (2012) The cancer stem cell subtype determines immune infiltration of glioblastoma. Stem Cells Dev 21(15):2753–2761

Bradshaw A, Wickremesekera A et al (2016) Cancer Stem Cells in Glioblastoma Multiforme. Front Surg 3:48

Bradshaw A, Wickremsekera A et al (2016) Cancer Stem Cell Hierarchy in Glioblastoma Multiforme. Front Surg 3:21

Carlsten M, Bjorkstrom NK et al (2007) DNAX accessory molecule-1 mediated recognition of freshly isolated ovarian carcinoma by resting natural killer cells. Cancer Res 67(3):1317–1325

Castriconi R, Dondero A et al (2007) Both CD133 + and CD133-medulloblastoma cell lines express ligands for triggering NK receptors and are susceptible to NK-mediated cytotoxicity. Eur J Immunol 37(11):3190–3196

Champsaur M, Lanier LL (2010) Effect of NKG2D ligand expression on host immune responses. Immunol Rev 235(1):267–285

Chitadze G, Bhat J et al (2013) Generation of soluble NKG2D ligands: proteolytic cleavage, exosome secretion and functional implications. Scand J Immunol 78(2):120–129

Chitadze G, Lettau M et al (2015) NKG2D- and T-cell receptor-dependent lysis of malignant glioma cell lines by human gammadelta T cells: Modulation by temozolomide and A disintegrin and metalloproteases 10 and 17 inhibitors. Oncoimmunology 5(4):e1093276

Chitadze G, Fluh C et al (2017) In-depth immunophenotyping of patients with glioblastoma multiforme: Impact of steroid treatment. Oncoimmunology 6(11):e1358839

Codo P, Weller M et al (2014) MicroRNA-mediated down-regulation of NKG2D ligands contributes to glioma immune escape. Oncotarget 5(17):7651–7662

Di Tomaso T, Mazzoleni S et al (2010) Immunobiological characterization of cancer stem cells isolated from glioblastoma patients. Clin Cancer Res 16(3):800–813

Fluh C, Hattermann K et al (2016) Differential expression of CXCR4 and CXCR7 with various stem cell markers in paired human primary and recurrent glioblastomas. Int J Oncol 48(4):1408–1416

Friese MA, Platten M et al (2003) MICA/NKG2D-mediated immunogene therapy of experimental gliomas. Cancer Res 63(24):8996–9006

Gasser S, Orsulic S et al (2005) The DNA damage pathway regulates innate immune system ligands of the NKG2D receptor. Nature 436(7054):1186–1190

Hattermann K, Held-Feindt J et al (2010) The chemokine receptor CXCR7 is highly expressed in human glioma cells and mediates antiapoptotic effects. Cancer Res 70(8):3299–3308

Hattermann K, Fluh C et al (2016) Stem cell markers in glioma progression and recurrence. Int J Oncol 49(5):1899–1910

Held-Feindt J, Hattermann K et al (2010) CX3CR1 promotes recruitment of human glioma-infiltrating microglia/macrophages (GIMs). Exp Cell Res 316(9):1553–1566

Ignatova TN, Kukekov VG et al (2002) Human cortical glial tumors contain neural stem-like cells expressing astroglial and neuronal markers in vitro. Glia 39(3):193–206

Jung TY, Choi YD et al (2013) Immunological characterization of glioblastoma cells for immunotherapy. Anticancer Res 33(6):2525–2533

Kmiecik J, Poli A et al (2013) Elevated CD3 + and CD8 + tumor-infiltrating immune cells correlate with prolonged survival in glioblastoma patients despite integrated immunosuppressive mechanisms in the tumor microenvironment and at the systemic level. J Neuroimmunol 264(1–2):71–83

Kreso A, Dick JE (2014) Evolution of the cancer stem cell model. Cell Stem Cell 14(3):275–291

Kruse V, Hamann C et al (2015) Human induced pluripotent stem cells are targets for allogeneic and autologous natural killer (NK) cells and killing is partly mediated by the activating NK receptor DNAM-1. PLoS One 10(5):e0125544

Lamb LS Jr, Bowersock J et al (2013) Engineered drug resistant gammadelta T cells kill glioblastoma cell lines during a chemotherapy challenge: a strategy for combining chemo- and immunotherapy. PLoS One 8(1):e51805

Lunemann A, Lunemann JD et al (2008) Human NK cells kill resting but not activated microglia via NKG2D- and NKp46-mediated recognition. J Immunol 181(9):6170–6177

Molinero LL, Fuertes MB et al (2002) Activation-induced expression of MICA on T lymphocytes involves engagement of CD3 and CD28. J Leukoc Biol 71(5):791–797

Nakamura K, Nakayama M et al (2013) Fratricide of natural killer cells dressed with tumor-derived NKG2D ligand. Proc Natl Acad Sci USA 110(23):9421–9426

Nausch N, Cerwenka A (2008) NKG2D ligands in tumor immunity. Oncogene 27(45):5944–5958

O'Connor ML, Xiang D et al (2014) Cancer stem cells: a contentious hypothesis now moving forward. Cancer Lett 344(2):180–187

Pende D, Rivera P et al (2002) Major histocompatibility complex class I-related chain A and UL16-binding protein expression on tumor cell lines of different histotypes: analysis of tumor susceptibility to NKG2D-dependent natural killer cell cytotoxicity. Cancer Res 62(21):6178–6186

Pereboeva L, Harkins L et al (2015) The safety of allogeneic innate lymphocyte therapy for glioma patients with prior cranial irradiation. Cancer Immunol Immunother 64(5):551–562

Raulet DH, Gasser S et al (2013) Regulation of ligands for the NKG2D activating receptor. Annu Rev Immunol 31:413–441

Salih HR, Antropius H et al (2003) Functional expression and release of ligands for the activating immunoreceptor NKG2D in leukemia. Blood 102(4):1389–1396

Salih HR, Holdenrieder S et al (2008) Soluble NKG2D ligands: prevalence, release, and functional impact. Front Biosci 13:3448–3456

Sottoriva A, Spiteri I et al (2013) Intratumor heterogeneity in human glioblastoma reflects cancer evolutionary dynamics. Proc Natl Acad Sci USA 110(10):4009–4014

Spreu J, Stehle T et al (2006) Human cytomegalovirus-encoded UL16 discriminates MIC molecules by their alpha2 domains. J Immunol 177(5):3143–3149

Stupp R, Hegi ME et al (2009) Effects of radiotherapy with concomitant and adjuvant temozolomide versus radiotherapy alone on survival in glioblastoma in a randomised phase III study: 5-year analysis of the EORTC-NCIC trial. Lancet Oncol 10(5):459–466

Vetter CS, Groh V et al (2002) Expression of stress-induced MHC class I related chain molecules on human melanoma. J Invest Dermatol 118(4):600–605

Watson NF, Spendlove I et al (2006) Expression of the stress-related MHC class I chain-related protein MICA is an indicator of good prognosis in colorectal cancer patients. Int J Cancer 118(6):1445–1452

Wolpert F, Tritschler I et al (2014) A disintegrin and metalloproteinases 10 and 17 modulate the immunogenicity of glioblastoma-initiating cells. Neuro Oncol 16(3):382–391

Wu J, Chalupny NJ et al (2003) Intracellular retention of the MHC class I-related chain B ligand of NKG2D by the human cytomegalovirus UL16 glycoprotein. J Immunol 170(8):4196–4200

Zeppernick F, Ahmadi R et al (2008) Stem cell marker CD133 affects clinical outcome in glioma patients. Clin Cancer Res 14(1):123–129